AD NUMBER
AD011322
CLASSIFICATION CHANGES
TO: unclassified
FROM: confidential
LIMITATION CHANGES
TO: Approved for public release, distribution unlimited
FROM: Distribution authorized to U.S. Gov't. agencies and their contractors; Administrative/Operational Use; 08 JUN 1953. Other requests shall be referred to National Aeronautics and Space Administration, Washington, DC 20330.
AUTHORITY
NASA TR Server website; NASA TR Server website

AD-

11322

CONFIDENTIAL

CONFIDENTIAL

Copy
RM L53E08

RESEARCH MEMORANDUM

A SUMMARY OF DATA ON THE DIVISION OF LOADS FOR VARIOUS WING-FUSELAGE COMBINATIONS

By Clarence L. Gillis

Langley Aeronautical Laboratory
Langley Field, Va.

NATIONAL ADVISORY COMMITTEE
FOR AERONAUTICS

WASHINGTON

June 8, 1953

NATIONAL ADVISORY COMMITTEE FOR AERONAUTICS

RESEARCH MEMORANDUM

A SUMMARY OF DATA ON THE DIVISION OF LOADS FOR VARIOUS WING-FUSELAGE COMBINATIONS

By Clarence L. Gillis

SUMMARY

A summary has been made of the available experimental data on division of normal-force loads between the wing and fuselage of aircraft. Comparison of the experimental values with theoretical calculations which include interference effects shows good agreement in general with the greatest differences occurring near a Mach number of 1.0. At high angles of attack, above the range of linear lift curves, the proportion of the total wing-fuselage load carried by the wing decreases and this effect occurs throughout the subsonic- and transonic-speed regions.

INTRODUCTION

The purpose of this paper is to summarize the presently available experimental data on division of normal-force loads between the wing and fuselage of aircraft configurations and to make comparisons with theoretical results. The experimental information presented herein was obtained by means of four different test methods: wind tunnels, free-fall models, rocket-propelled models, and airplane flight tests. The data were measured by various combinations of pressure distributions, strain gages, internal balances, and accelerometers. Further details on the methods of measurement can be found in the reference reports. Most of the data are presented in the form of the rate of change of wing normal-force coefficient with wing-fuselage normal-force coefficient with both coefficients being based on the same reference area. In those cases where a tail surface was present during the tests, the tail load was subtracted from the data to obtain wing-fuselage load.

METHODS OF ESTIMATION

Several means have commonly been used to estimate the division of lift or normal-force loads between the wing and fuselage, as illustrated in figure 1. The simplest scheme for estimating the proportion of lift carried by the wing is to take the ratio of the exposed wing area to the total wing area which is equivalent to assuming that there are no aerodynamic induction effects and that the span loading is not affected by the addition of a fuselage. A somewhat more refined method is to obtain the span loading for the wing without a fuselage and to form the ratio of the load on the exposed wing to the load on the entire wing as if it were unaffected by the presence of the fuselage. This method accounts for aerodynamic induction effects on the isolated wing and thus might be expected to account for the major effects of taper and sweepback.

In actuality, the load buildup on the wing-fuselage combination is more complex than indicated by either of these simple concepts. In addition to the loads that would occur on the isolated wing and fuselage, as indicated by the symbols F and W in figure 1, increments of load exist on the fuselage caused by the presence of the wing $F(W)$ and on the wing caused by the fuselage $W(F)$. Both the experimental and theoretical results presented herein include these interference effects.

The theoretical results at subsonic speeds follow a method outlined in reference 1 in which a combination of theoretical results from Multhopp, Weissinger, DeYoung, and Lennertz is used. For supersonic speeds theoretical methods have been presented in references 2 and 3 by Nielsen and his associates and in reference 4 by Tucker. All these results apply to supersonic speeds and wings with trailing edges that are not swept back. Recently, Nielsen has shown that his theory is valid at subsonic and transonic speeds also and is, in fact, equivalent to the subsonic theory outlined in reference 1. Tucker has extended his theoretical analysis (unpublished) to cover wings with sweptback trailing edges at supersonic speeds. Although the simpler methods of estimating the division of load between the wing and fuselage may give very good results for some cases, there is little reason to use these methods in any case because of the relative ease of applying the theoretical methods which include all the interference effects. Convenient charts have been set up by both Nielsen and Tucker; thus, the computation of the wing and fuselage loads by either method is only a matter of minutes.

RESULTS

Figure 2 shows data that have been obtained on low-aspect-ratio unswept wings to show the effect of relative wing-fuselage size. The

abscissa in this case is the ratio of fuselage diameter to wing span. The ordinate $dC_{N_W}/dC_{N_{WF}}$ is the rate of change of wing normal-force coefficient with wing-fuselage normal-force coefficient and represents the proportion of the total wing-fuselage load that is being carried by the wing over that part of the lift range where linearity exists. The distance above the curve to the ordinate 1.0 is, of course, the proportion being carried by the fuselage.

The data on the left side of figure 2 are from reference 1 and were obtained in the Ames 7- by 10-foot tunnel at a Mach number of 0.25 on a wing of aspect ratio 3 with three sizes of body. The tests included both changes in angle of attack of the entire configuration (indicated by squares) and changes in wing incidence (indicated by circles). It can be seen that the theoretical calculations agree very well with the experimental results for both variable incidence and variable angle of attack. An area-ratio and a load-ratio estimate give fairly good results for the variable angle-of-attack case.

On the right side of the figure are shown data, from reference 5, at three supersonic speeds from the Langley 9-inch supersonic tunnel. Variations in the ratio of diameter to span were obtained by altering the wing span so that the aspect ratio also varied. Theoretical calculations from both Tucker and Nielsen are shown. Both sets of calculations indicate the correct variation with the diameter-to-span ratio but Tucker's results appear to predict the variation with Mach number somewhat better.

Figure 3 shows a summary of the effects of Mach number on unswept wings of aspect ratio 3. The points represented by symbols were taken from figure 2. The short solid curve at transonic speeds was obtained at the Ames Laboratory from a free-fall model. The fuselage lift on the free-fall model was obtained from pressure measurements in the vicinity of the wing; thus, any lift on the nose of the fuselage is not included in the data and has also been omitted from the comparable theoretical results. The Nielsen theory is independent of Mach number and agrees very well with the experimental data but the Tucker theory gives somewhat higher values. The longer solid curve is experimental data obtained at the Langley Laboratory (ref. 6) from a rocket-propelled model. Values of both theoretical calculations are higher than the experimental values, but the Nielsen theory, again independent of Mach number, gives somewhat better agreement, particularly with the subsonic experimental data. Both the experimental data and the Tucker theory indicate some decrease in the proportion of load carried by the wing as the Mach number increases at low supersonic speeds.

Turning now to swept wings, figure 4 presents data measured on the full-scale Douglas D-558-II airplane at Mach numbers from 0.4 to 1.5.

The curve indicates that the proportion of load carried by the wing decreases above a Mach number of 0.8 and then increases again as supersonic speed is attained. The theoretical values are again somewhat higher than the experimental values.

Figure 5 presents a summary of available data on wings with 45° of sweepback. Information on aspect-ratio-4 wings has been obtained in the Langley 8-foot and 16-foot transonic tunnels (refs. 7 and 8). The results from the two tunnels agreed very well, and the single line shown represents both sets of data. Data at the higher Mach numbers were obtained from two rocket-propelled models (ref. 9) which were geometrically identical but had different wing stiffnesses. The wings differed in stiffness by a factor of 3 since the wing labeled rigid was solid steel and the flexible wing was solid aluminum. Over most of the Mach number range where data were obtained, the flexible wing carries a slightly smaller proportion of the wing-fuselage load than does the rigid wing. This does not mean that the effect of wing flexibility on lift-curve slope is small. The reduction in lift-curve slopes due to flexibility was about 5 to 7 percent for the relatively rigid wing and about 15 to 20 percent for the flexible wing but, when the ratio of the wing to the wing-fuselage slope is taken, the difference due to flexibility is only a few percent as shown here. In this case, the agreement between theory and experiment is very good. All the experimental data indicate a slight increase in the proportion of load carried by the wing in the Mach number region near 1.0.

Data on aspect-ratio-6 wings have been obtained on two free-fall models, one having a plane wing and one a cambered-and twisted wing, and on one rocket-propelled model. These data also indicate a general increase in the proportion of load carried by the wing in the transonic region. The theoretical results indicate the same trends with Mach number as the experimental data but give smaller absolute values. Although the Nielsen theory is not strictly applicable to swept wings, the error involved in its use is small and a calculation made for the free-fall models gave a value of 0.81 which agrees very well with the measurements.

Figure 6 presents data that have been obtained on 60° swept wings from the full-scale Bell X-5 airplane and a rocket model having the X-5 wing (ref. 10). The wing plan form on the model differed from that on the airplane in that it was not rounded at the trailing-edge tip and the leading edge at the root did not simulate the nonmoving portion of the full-scale variable-sweep wing. Reference to the two area ratios indicates that the data for the X-5 airplane should be higher than for the two sets of experimental data is not known but it may be associated with the differences in fuselage shape and wing-root fairing. The theoretical and experimental results are in very good agreement.

The experimental information available on triangular-wing configurations is not so extensive as that on unswept and swept wings. Figure 7 presents data obtained in the Ames 7- by 10-foot tunnel on the effects of fuselage size with aspect-ratio-2 triangular wings at a Mach number of 0.25. The ratio of the body diameter to wing span was varied by using two bodies and three wings. The results obtained when the wing incidence was varied were fairly linear and agreed well with theory. When the angle of attack of the entire configuration was varied, the data were not linear and two values of slope are shown here, one being the slope at an angle of attack of 0° and the other being the slope of a line drawn through $\alpha = 0^\circ$ and $\alpha = 10^\circ$. The theoretical calculations agree better with the slopes measured between 0° and 10°. It can be seen that a simple area ratio fails by a wide margin to predict the relative proportions of load carried by the wing and fuselage. The load-ratio estimation gives much better agreement but is still not so good as the theoretical calculations.

Figure 8 presents information that has been obtained on two triangular-wing configurations at transonic and low supersonic speeds. The aspect-ratio-4 wing was flown on a free-fall model and the aspect-ratio-2.31 wing was flown on a rocket-propelled model (ref. 11). Again, the simple area ratio fails by a wide margin to predict the experimental results. Both the Nielsen and Tucker theoretical methods give fairly good agreement with the measured data.

Up to this point only data at low angles of attack over what is usually a linear range have been considered. Critical load conditions may also occur at high angles of attack where flow separation exists and theoretical calculations no longer apply. Although data at high angles of attack are not as plentiful as for the low angle-of-attack range, some information on a number of configurations has been obtained and is summarized in figures 9 and 10.

The information in figure 9 is presented as wing normal-force coefficient against total airplane normal-force coefficient and, in all cases, extends to angles of attack above the pitch-up boundary. Data have been obtained at supersonic speeds for the D-558-II airplane and the first plot in figure 9 shows these data. The Mach number for the maneuver from which these data were obtained started at about 1.45 and decreased to 1.04 as the higher angles of attack were attained. The data indicate that the linear range extends to a wing normal-force coefficient of about 0.7 above which the proportion of the load carried by the wing decreases considerably as the angle of attack increases, similar to the behavior at lower speeds reported previously (ref. 12). The dashed line is an extension of the linear rarge to present a comparison with the measured curve.

Similar data have been obtained on three rocket-model configurations as shown in the other plots in figure 9 and indicate the same effect of a decrease in the proportion of load carried by the wing at the higher angles of attack. Two models having 45° swept wings of aspect ratio 4, one with a rigid wing and one with a flexible wing, as discussed previously, entered the pitch-up region at slightly different Mach numbers but gave similar curves, the linear region extending to a C_{N_W} of about 0.6. Similar results at a Mach number of 0.90 are shown for a rocket model with a 60° triangular wing with the linear range extending to a C_{N_W} of 0.6. Another rocket model having a 45° swept wing of aspect ratio 6 exceeded the linear range three times between Mach numbers of 0.69 and 0.82, and the data all plot on the single curve shown. Although this model attained lift coefficients above the pitch-up boundary for the wing, it did not experience any violent pitch-up maneuvers, probably because of the location of the horizontal tail below the wing. In general, the departure of the curves of C_{N_W} against C_{N_A} from linearity occurred at about the same angles of attack as the departure from linearity of the basic lift curves for these configurations. The measured angles of attack at the breaks in the curves were about 13° for the D-558-II airplane, 9° for the aspect-ratio-4 models, 14° for the delta-wing model, and 8° for the aspect-ratio-6 model.

The data on the configurations in figure 9 were obtained at only a few Mach numbers. A more extensive coverage of the Mach number range is available on the two configurations shown in figure 10. The test results shown at the top of the figure for a 45° swept wing of aspect ratio 4 were run in the Langley 8-foot transonic tunnel (ref. 7). Only a few angles of attack were tested so it is not possible to plot continuous curves as in figure 9; however, the ratio of the wing normal-force coefficient to the wing-fuselage normal-force coefficient is shown in figure 10 to indicate the effects of high angles of attack. Only very small differences in this ratio occurred for the small angles of attack, indicating the linearity, and only one curve is shown here for 4° and 8° angles of attack. For 20° angle of attack, however, a consistently smaller proportion of the load was carried by the wing over the Mach number range from 0.60 to 1.13.

On the full-scale X-5 airplane, the Mach number range from 0.70 to 1.00 has been covered fairly completely. The curves shown here represent less than half the data that have been obtained. Again, the decrease in the wing load above the linear range at all Mach numbers is noted. Of particular interest in this case, also, is the small range of linearity, the break in the curves occurring at a wing normal-force coefficient of about 0.35 at a Mach number of 0.70 and decreasing to 0.30 at a Mach number of 1.00. On this configuration the break in the curves of C_{N_W}

against C_{N_A} occurred fairly consistently at an angle of attack about 1° to 3° lower than the break in the lift curve for the complete airplane. A brief effort at correlating the data for the configurations shown in figures 9 and 10 indicates that the ratio of the lift-curve slope $dC_N/d\alpha$ above the break in the curves to the slope below the break is roughly 30 percent less for the exposed wing than for the complete airplane.

CONCLUDING REMARKS

To summarize, it appears that the division of normal-force loads at low angles of attack between the wing and fuselage of aircraft can be fairly well calculated by theoretical methods except possibly at Mach numbers just above 1.0. The theoretical methods have been reduced to simple procedures so that only a matter of minutes is necessary for the calculations for one configuration. Although the simple area ratio and load ratio used for approximate estimations may give fairly good results for wings that do not have much taper, there is little reason for using these simple methods in any case because of the simplicity of the theoretical calculations which account for all interference effects. Based on the data shown herein, the theory of Nielsen appears to give a closer prediction of experimental results at the low supersonic Mach numbers, whereas, the theory of Tucker may give a somewhat better prediction of the results at higher Mach numbers, although insufficient data are available to establish firmly this conclusion.

The linear range, to which the preceding statements apply, extended to wing normal-force coefficients varying from 0.7 to 0.3 depending on aspect ratio and sweepback. At higher angles of attack, above the range of linearity, the proportion of the normal force carried by the wing becomes progressively less as the angle of attack increases, as shown by a variety of wings including a 60° delta wing and swept wings ranging from 35° to 60° sweepback. As indicated by two swept-wing configurations, this decrease in proportionate wing load at high angles of attack occurs generally throughout the subsonic- and transonic-speed regions.

Langley Aeronautical Laboratory,
National Advisory Committee for Aeronautics,
Langley Field, Va., April 28, 1953.

REFERENCES

1. Hopkins, Edward J., and Carel, Hubert C.: Experimental and Theoretical Study of the Effects of Body Size on the Aerodynamic Characteristics of an Aspect Ratio 3.0 Wing-Body Combination. NACA RM A51G24, 1951.

2. Nielsen, Jack N., Katzen, Elliott D., and Tang, Kenneth K.: Lift and Pitching-Moment Interference Between a Pointed Cylindrical Body and Triangular Wings of Various Aspect Ratios at Mach Numbers of 1.50 and 2.02. NACA RM A50F06, 1950.

3. Nielsen, Jack N., and Kaattari, George E.: Method for Estimating Lift Interference of Wing-Body Combinations at Supersonic Speeds. NACA RM A51J04, 1951.

4. Tucker, Warren A.: A Method for Estimating the Components of Lift of Wing-Body Combinations at Supersonic Speeds. NACA RM L52D22, 1952.

5. Coletti, Donald E.: Investigation of Interference Lift, Drag, and Pitching Moment of a Series of Rectangular Wing and Body Combinations at Mach Numbers of 1.62, 1.93, and 2.41. NACA RM L52E26, 1952.

6. McFall, John C., Jr., and Hollinger, James A.: Longitudinal Stability, Control Effectiveness, and Drag Characteristics at Transonic Speeds of a Rocket-Propelled Model of an Airplane Configuration Having an Unswept Tapered Wing of Aspect Ratio 3.0 and NACA 65A004.5 Airfoil Sections. NACA RM L52L04, 1953.

7. Loving, Donald L., and Williams, Claude V.: Aerodynamic Loading Characteristics of a Wing-Fuselage Combination Having a Wing of 45° Sweepback Measured in the Langley 8-Foot Transonic Tunnel. NACA RM L52B27, 1952.

8. Hallissy, Joseph M., and Bowman, Donald R.: Transonic Characteristics of a 45° Sweptback Wing-Fuselage Combination. Effect of Longitudinal Wing Position and Division of Wing and Fuselage Forces and Moments. NACA RM L52K04, 1953.

9. Vitale, A. James: Effects of Wing Elasticity on the Aerodynamic Characteristics of an Airplane Configuration Having 45° Sweptback Wings As Obtained From Free-Flight Rocket-Model Tests at Transonic Speeds. NACA RM L52L30, 1953.

10. Vitale, A. James, McFall, John C., Jr., and Morrow, John D.: Longitudinal Stability and Drag Characteristics at Mach Numbers From 0.75 to 1.5 of an Airplane Configuration Having a 60° Swept Wing of Aspect Ratio 2.24 As Obtained From Rocket-Propelled Models. NACA RM L51K06, 1952.

11. Peck, Robert F., and Mitchell, Jesse L.: Rocket-Model Investigation of Longitudinal Stability and Drag Characteristics of an Airplane Configuration Having a 60° Delta Wing and a High Unswept Horizontal Tail. NACA RM L52K04a, 1953.

12. Mayer, John P., and Gillis, Clarence L.: Division of Load Among the Wing, Fuselage, and Tail of Aircraft. NACA RM L51E14a, 1951.

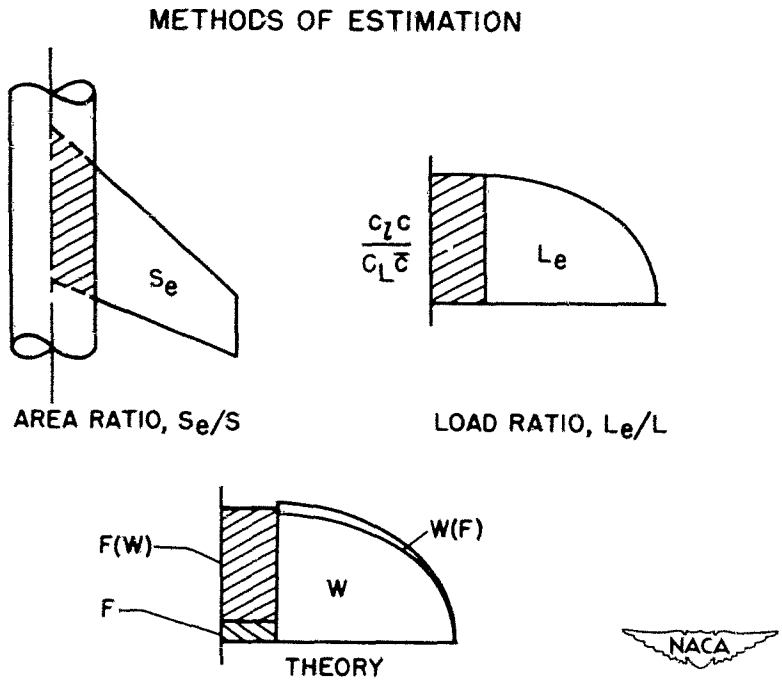

Figure 1.

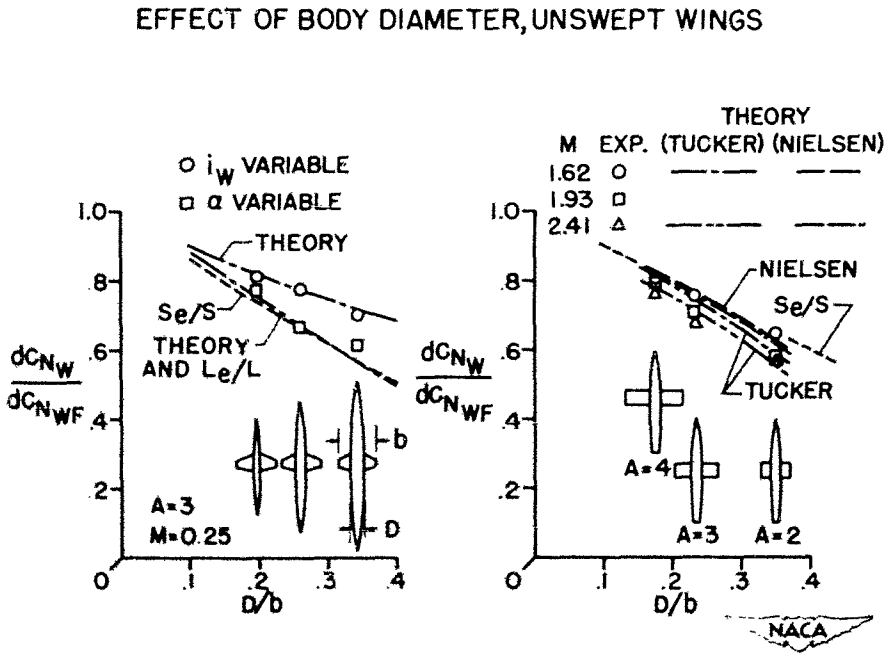

Figure 2.

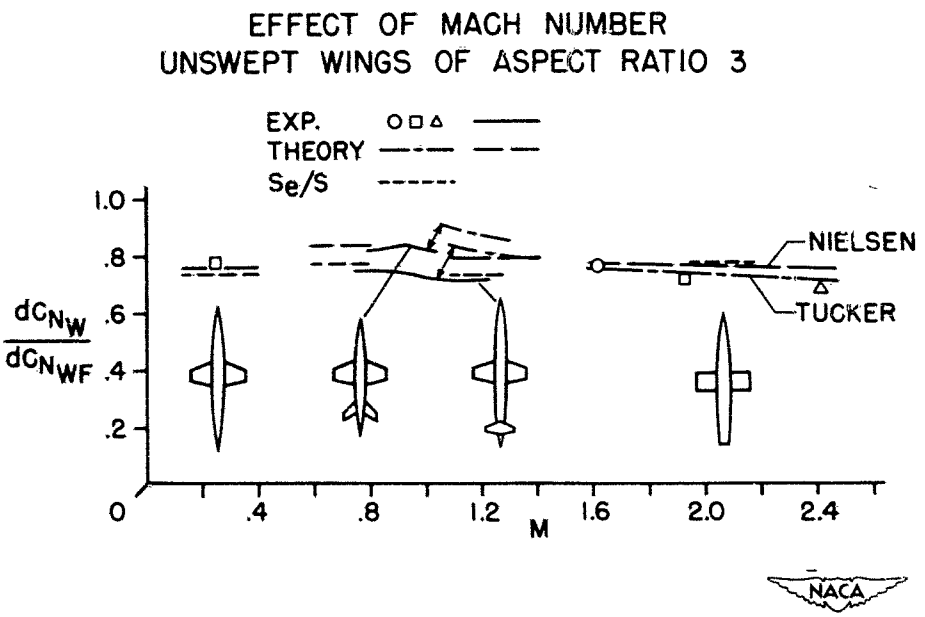

Figure 3.

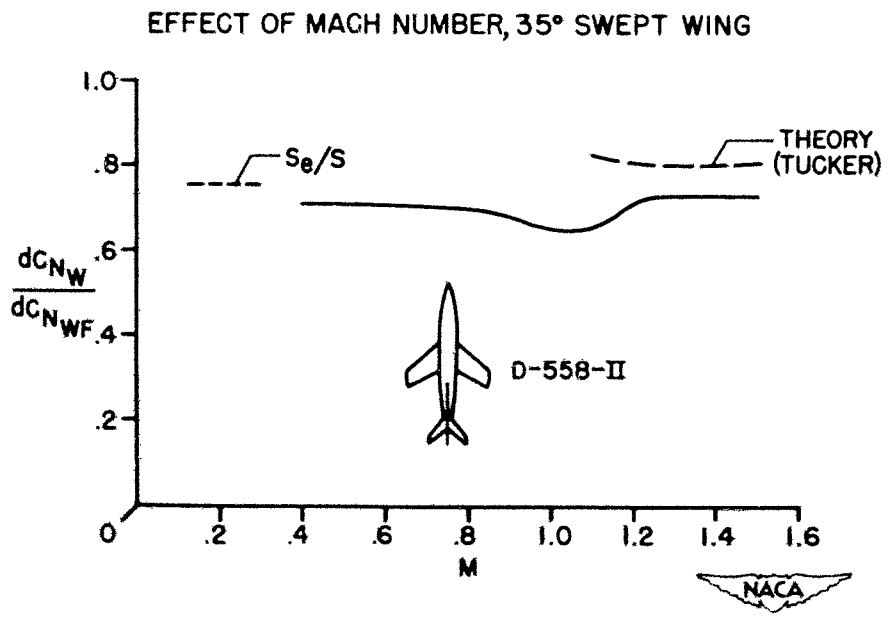

Figure 4.

EFFECT OF MACH NUMBER, 45° SWEPT WINGS

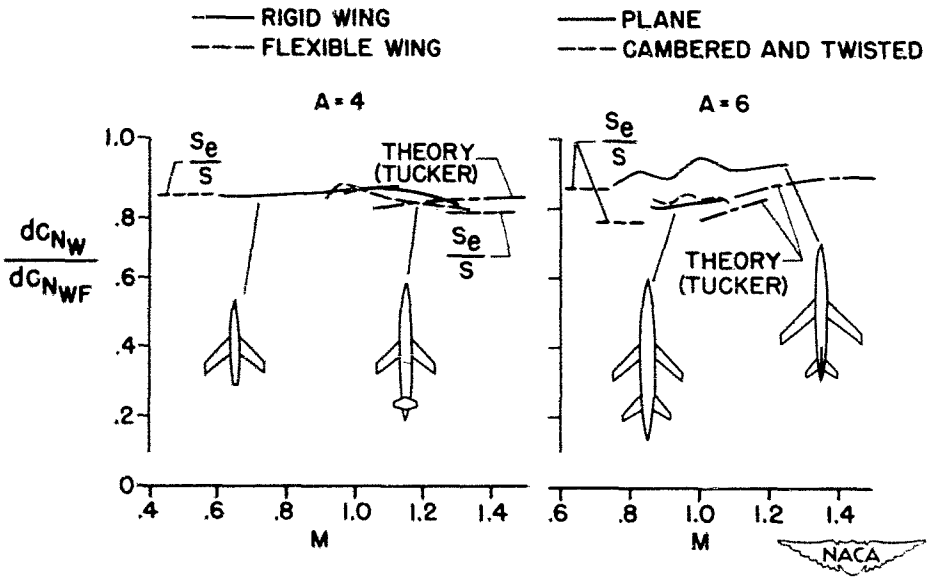

Figure 5.

EFFECT OF MACH NUMBER, 60° SWEPT WINGS

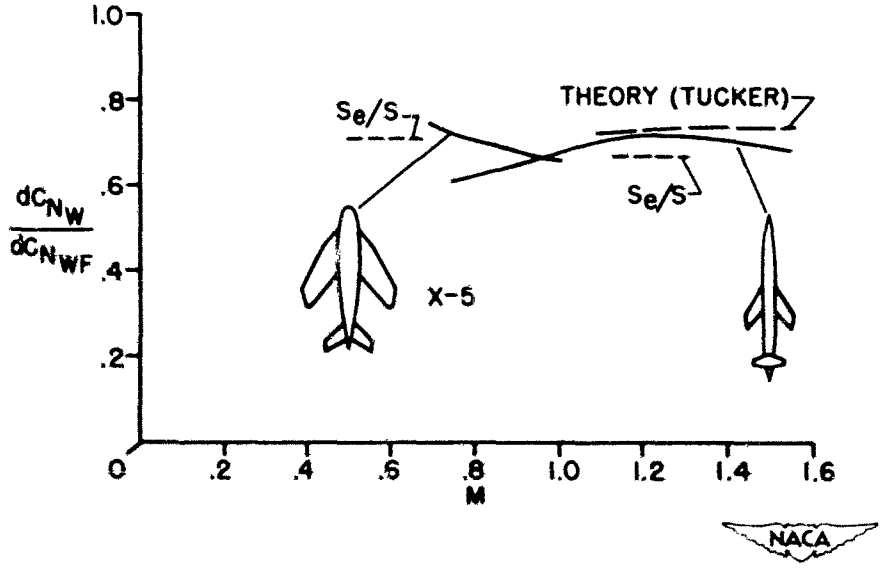

Figure 6.

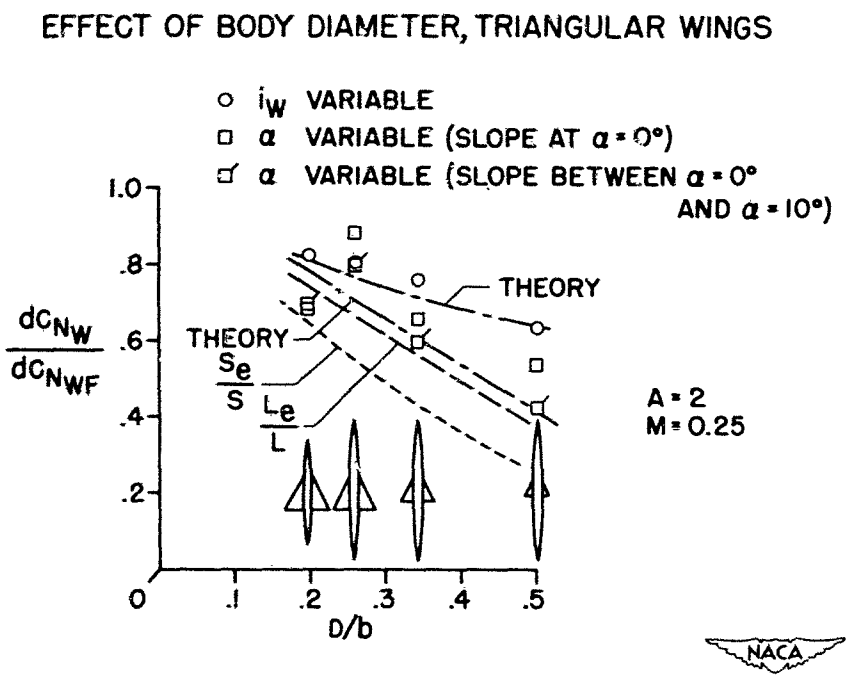

Figure 7.

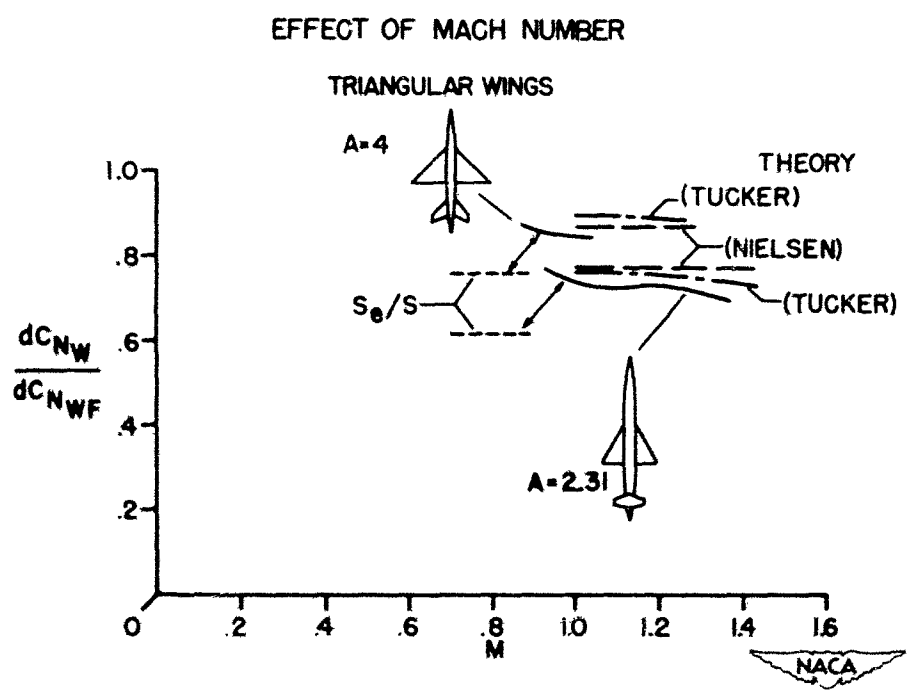

Figure 8.

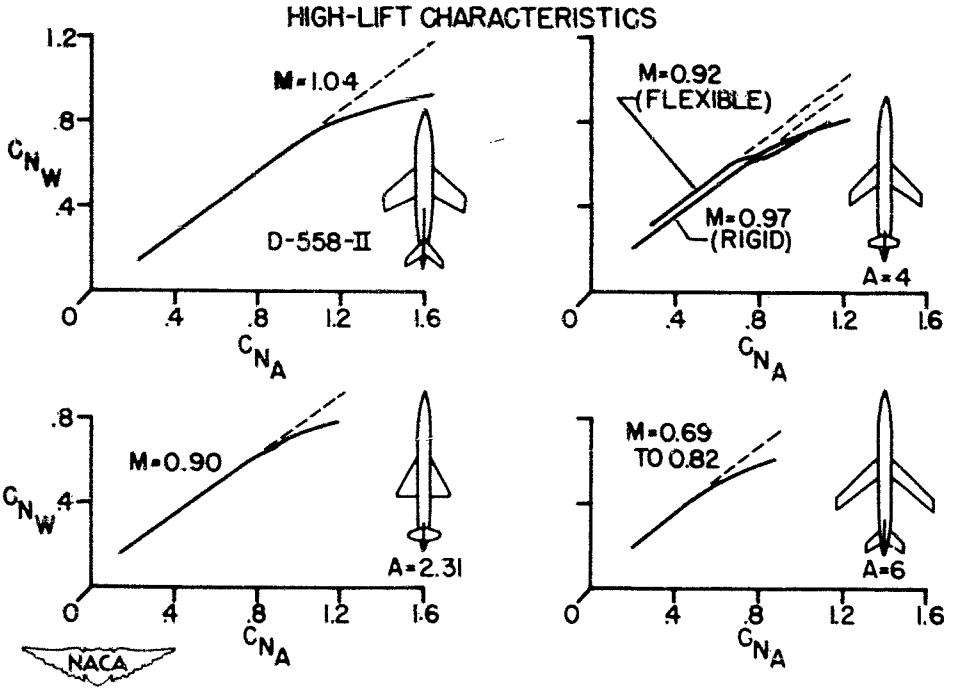

Figure 9.

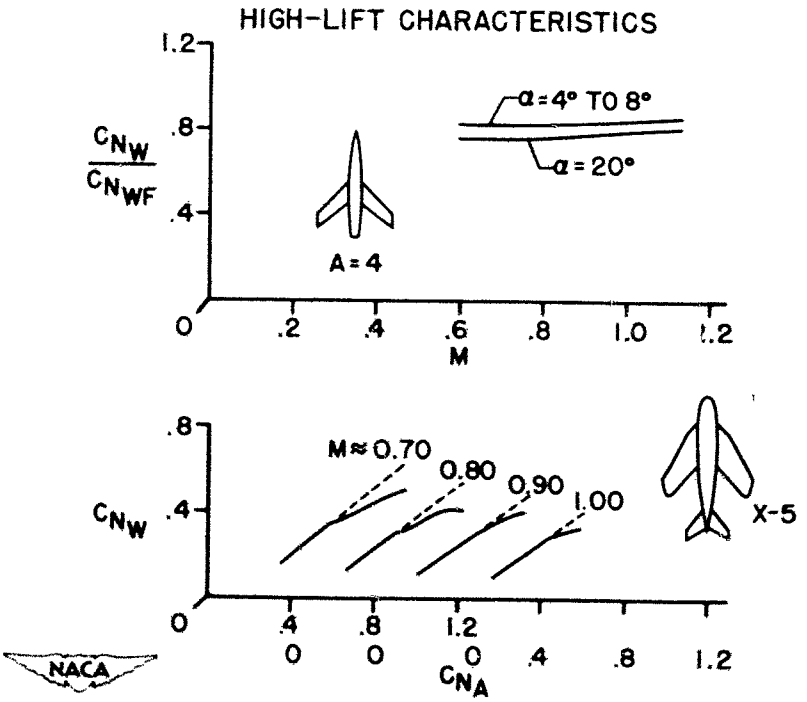

Figure 10.

NACA-Langley - 8-8-53 - 226